IJNRD.ORG ISSN : 2456-4184
INTERNATIONAL JOURNAL OF NOVEL RESEARCH AND DEVELOPMENT (IJNRD) | IJNRD.ORG
An International Open Access, Peer-reviewed, Refereed Journal

APPLICATION OF PID BASED TEMPERATURE CONTROLLED AUTOMATED ROBOTIC BASED GARRI FRYER

[1] Matthew O. Akusu, [2] Kaiser I. Amuche
[12]Senior officer,
[12]Department of Electrical and Electronics Engineering,
[12] Petroleum Training Institute, Effurun, Nigeria.

Abstract : Garri frying being the most important unit activity in the cassava to garri conversion process. This processing stage, which consists of a combination of simultaneous cooking and drying procedures, has a significant impact on the final product's quality. In local garri frying, the effect of heat and smoke on the local human fryers and the uncertainty of the homogeneous grits stirring and timely grits evacuation before burning, has necessitated a need for an intelligent garri fryer. This work makes use of the PID controller with variable gain parameters for the Proportional gain (P), Integral gain (I) and Derivative gain (D). The temperature is varied from 0℃ to 100℃ for the first 10 minutes and 100℃ to 200℃ for the next 10 minutes, which ensured a 12% moisture content when cold. This work is realized in a simulation set, using a two-degree-of-freedom controlled robotic arm, programed on Arduino uno microcontroller to move and conduct operations in Matlab Simulink environment. Solidworks is used for the computer-aided design, and the frame is made with AUTODESK computer-aided design software. This temperature controlled robotic arm is created to reduce human efforts, frying hazards, ensure a uniform grits combination, and perform rapid evacuation. The result of the simulation of this scheme shows; the controlled autonomous ability to routinely monitor garri quality using a temperature regulated approach to autonomously observe the system frying cycle to completion to form edible garri grits. The PID was manually tuned and the optimal tuned gain parameters were presented as P = 0.9, I = 2, D = 0.8. The development of this PID based temperature controlled autonomous robotic arm for frying garri will help to reduce the risk of human involvement in garri frying, improve the yield and quality of the gari production and improve exportation of garri to other countries.

IndexTerms **- Robotics, Food Processing, Garri, Garri Processing, Kinematics**

I. INTRODUCTION

Garri is a cassava-based product that is popular in Nigeria, as well as the rest of the West African coast and Brazil. It's a pre-gelatinized grit with particle sizes ranging from less than 10 micrometers to more than 2000 micrometers (Onokwai et al., 2019, Ndife, 2019 and Onu, 2020). Garri production involves series of unit operations, such as; harvest and sort your cassava to get the best, peel the cassava roots, wash and clean the cassava root, grate the cassava roots into a mash, ferment the Cassava Mash to Remove Hydrocyanic Acid, press the cassava sack to drain the water in the Garri, sifting the wet cake into grits, fry the grits to form edible Garri, spread the Garri in a thin layer and allow it to cool, sieve or grind the Garri to break larger granules, and pack the Garri in airtight bags and store properly (Miriam, 2017, Ndife, 2019, Onu, 2020, Samuel et al., 2021 and Dike et al., 2022). Among these Garri processing units, the frying operation is the most important unit activity in the garri production process since it influences the quality of the end product (Ndife, 2019, Samuel et al., 2021 and Ovat et al., 2021). Garri frying entails repeatedly pressing, scraping, swirling and sifting cassava mush over a hot plate at 120 to 200℃, and final storage or serving of the process garri as meal (Dike et al., 2022). However, when it comes to the application of human efforts and skills in the garri production processes, the frying of the grits into edible form (Garri) is often the most critical part, as it involves human exposure to noxious gasses, monotony in grits stirring, uncertain assumption of the frying temperature, inexperience among learners, poor homogeneity of the fried mixture, and so on. This has prompted research into the development of modern garri production and frying schemes, in order to alleviate the numerous burdens borne (Miriam, 2017 Nwadinobi et al., 2019, Adesope et al., 2020, Kayode et al., 2021 and Charles Nnaji & Chigozie Akanno, 2022), A PID based temperature-sensing autonomous robotic arm for frying garri is presented in this paper. This is capable of autonomously frying and homogeneously mixing the garri grits at a moisture-tolerable temperature of 200°C, which will be measured automatically to determine the moisture level of less than 12 percent.

II. REVIEWED LITERATURE

There are only a handful mechanized gari processing plants in the Nigerian market today. As a result, Nigerian engineers and manufacturers have created some new designs and upgrades to address issues with existing models on the market. For the whole fabrication of soft fabric shoe tongues, Tsai et al., (2020), designed an automatic robotic arm production line using a cyber-physical system artificial intelligence (CPS-AI) architecture. The Deep-Q reinforcement learning (RL) method was offered as a way of improving manufacturing process control, while the convolutional and long short-term memory artificial neural network was created to improve action speed. Through repeated training, this technique allows a robotic arm to understand the precise picture feature spots of a shoe tongue, improving manufacturing accuracy. Different network architectural parameters were tried for validation, and the test convergence accuracy was found to be enhanced.

Vestartas & Weinand, (2020), demonstrated a raw-wood fabrication workflow that included an industrial robot arm and a laser scanner. The study takes place in a Swiss mountain forestry setting, where natural wood could be used locally instead of depending on highly centralized timber industries. While local sawmills use normal processing equipment to turn raw timber into standard beams and boards, a fully automated application might use timber in its original state for building. The study presents a digital fabrication workflow that combines an industrial robot arm with laser scanning to adapt timber joinery toolpaths to irregular raw wood such as straight, twisted, and forked tree trunks. In terms of calibration, pointcloud processing, robotic control communication time, and accuracy, the scanning method was compared. The findings revealed that robotic cutting and scanning can be performed interchangeably and at a faster rate.

Al-Faraj et al., (2021) conceived, constructed, and implemented a CNN-based machine learning system for successfully identifying items labelled with English alphabets and sorting them in the correct order depending on user input. It is made up of a hardware module that houses a robotic arm that is controlled by a Raspberry Pi microcontroller. The software module was built using a CNN-based image identifier model that was trained on a local dataset of 3898 images of English alphabets rotated at various angles. Based on the model trained across 120 epochs, the experimental findings show training and validation accuracies of 99.06 percent and 98.79 percent, respectively. In addition, our system was able to sort and arrange the alphabets with the required precision.

Wang et al., (2021) presented a robotic arm system for object collection and transmission between stations, that can rapidly generate a large database of archaeological artifacts. This was validated in a simulation block-set, using high-resolution models of sherds. In other contexts, the system may help to expand the use of automation in materials handling, parts sorting, and more.

Pradhan et al., (2021) used computer vision to provide a generalized, holistic solution for robotic arm handling of manufactured components in an industrial setting. These were scenarios in which a large number of manufactured parts were travelling over a conveyor belt at random locations and orientations while being manipulated by various robotic arms. All stages of the framework have particular, validated solutions, as well as some alternative techniques based on the literature research. In the data interpretation stage, 3D point clouds and object detection models were employed to offer valuable information such as object number, location, velocity, and orientation. The full-scale, cohesive system was put to the test, and the solutions to each stage demonstrated that such a system could be implemented in an industrial setting.

Ali et al., (2022), described the model, design, and building of an Arduino-based robotic arm that can operate over a long distance and is controlled by a mobile app. A robotic arm with six degrees of freedom was conceived and implemented. The Arduino-controlled design takes commands from the user's mobile application via Bluetooth-based wireless controlling signals. The arm was made up of five rotating joints and an end effector, with the servomotor providing rotary motion. The performance of the developed robotic arm was recommended to be optimal.

Krishnaraj Rao et al., (2022), used a Machine Learning technique to propose and demonstrate the design and operation of an automated robotic arm. For object identification and traversal, the study employs a Machine Learning technique, which is implemented with the TensorFlow package for better and more accurate results.

Ghodki, (2022), conceived and constructed a robotic arm system to serve as a hardware prototype of a biomass conveyor system based onmaster–slave electric motors that was employed under normal working settings without overheating. The system's hardware prototype used master–slave electric motors for a robotic arm controlled by an integrated controller to automatically swap conveyor motors with one another. When compared to traditional energy-based mains supply, the system is self-sufficient, allowing it to harvest more energy from solar sources, resulting in an 11.38 percent increase in energy. Solar energy-based energy savings were reported to be 52.69 percent higher than conventional energy-based energy savings of 47.31 percent.

There has been a lot of research on the usage of robotic arms for other applications. However, there hasn't been any research into its application to Garri manufacturing. This paper's concept revolves around a methodical approach to automating the frying process for Garri production. This paper is focused on the design and simulation of a temperature-controlled robotic arm for frying garri.

While several kinds of research have been carried out on the use of robotic arms for some applications, there hasn't been any recorded research work on its application to Garri production. The concept of the project borders around a systematic approach

involving the automation of the frying process for Garri production, with temperature and humidity sensing abilities. This work focused on the design and simulation of a robotic arm for garri frying.

III. MATERIAL AND METHOD

The Arduino Uno microprocessor, potentiometers, servomotors, temperature sensor, power adaptor, and the arm-frame are all required for the Robotic Arm to function. The Arduino IDE is required for programming the microcontroller, as well as SOLIDWORKS for computer-aided design. AUTODESK computer-aided design was used to create the frame. A prototype 3D design is built using this method to illustrate the robotic arm's frame build-up. Dassault Systems developed SOLIDWORKS, a solid modeling Computer-Aided Design (CAD) software. Along with the 3D design, 2D kinematic sketches were generated, which would eventually aid in the mathematical modeling of the robotic arm.

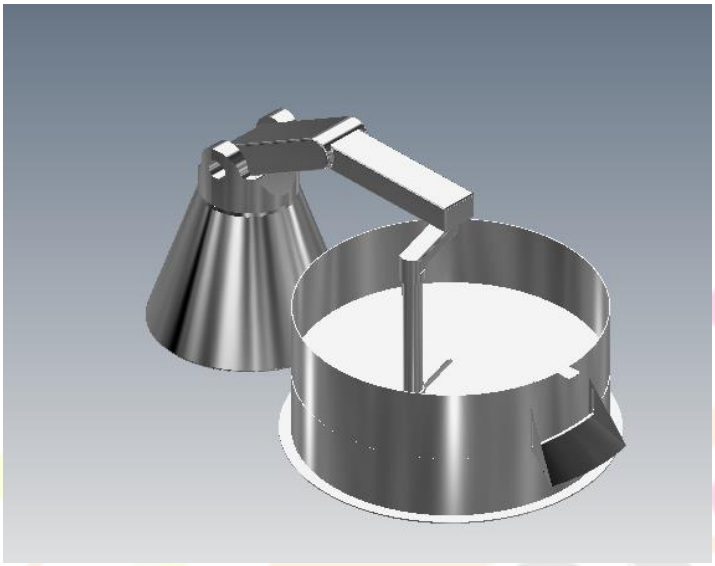

Figure 3.1 3D Side Model

The board contains an open-source program (IDE) for uploading commands to the ATmega 328p chip, and it uses an Arduino Uno as its microcontroller. Meanwhile, the purpose of this sub-handing is to emphasize the connection between the Arduino software and the hardware board, as well as other components that are connected to it (Onu, 2020; Ali et al., 2022).

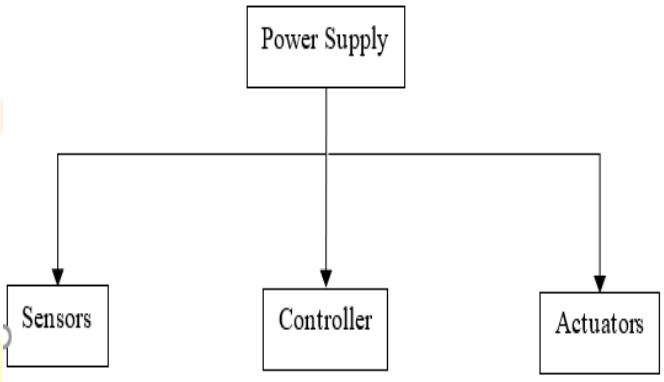

Figure 3.2 Block diagram of controller

This robot is meant to work in an XYZ Cartesian Coordinate System, homogeneously stirring cassava flakes within the given Cartesians until the installed sensor parameters are reached. The procedure will consist of just following sets of commands as they are entered into the Arduino IDE (Wu et al., 2021).

3.1 Initialization And Control

The initialization phase for an autonomous system establishes standards that other blocks of commands rely on. The initialization process for a system that meets the criteria for autonomy will involve the system flexing its joints to determine its degree of freedom (Ali et al., 2022). Receive a primary condition check of the heating object, as well as humidity and temperature readings from the garri flakes pan. The system will either proceed to commence control or refuse the command due to unfulfilled criteria after acquiring the essential parameters (Falanga et al., 2020). The flowchart below shows how this works.

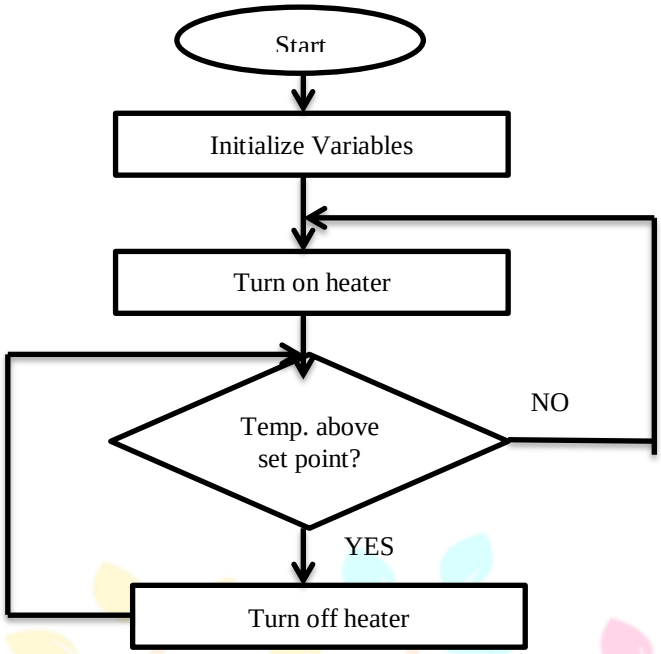

Figure 3.3 Flowchart of the temperature control algorithm

3.2 Description Of The Fryer Robot

The robot is designed to run on its own for a cycle period of around 20 minutes. Each cycle begins with the manual addition of material to the frying pot. It consists of two revolute joints and has two degrees of freedom (2 DOF). As a result, it is known as a 2R robot. The robot turns to a 90-degree angle for operation, ensuring that the paddle makes uniform contact with the frying pot's base. To simulate the stirring of the cassava grits, the controller actuates the movement of the robot in an intermittent 360-degree clockwise and counter-clockwise rotation.

The heating system operates at 75°C during the first 10 minutes of operation. The grains gelatinize throughout this time of operation. The frying process necessitates a higher temperature; therefore the controller raises the temperature to 200°C for the following 10 minutes. Following that, the heater is switched off. A user is prompted to open the discharge chute via an alarm. The robotic paddle then moves in a clockwise/counter-clockwise rhythm for 60 seconds, allowing the fried garri to be discharged more easily. The robot arm returns to its default 90-degree position after the time limit has expired, allowing another processing cycle to begin.

3.3 Robot Fryer Dynamics

Unlike kinematic analysis, dynamic analysis of the robot involves analysis of forces developed on the robot fryer in relation to the joint variables and dimensional parameters of the robot. In this work, the Euler-Lagrange method of analysing robot dynamics was applied. It involves computing the kinetic (K_E) and potential (P_E) energies on the fryer arm in order to determine the Lagrangian ($\mathcal{L}$) of the system. Thus, the motion of the robotic system is given by the nonlinear equation (3.1):

$$F = B(\ddot{q}) + C(\dot{q}, q) + g(q) \qquad (3.1)$$

Where:

$$F = \begin{bmatrix} F_{\theta_1} \\ F_{\theta_2} \end{bmatrix} \qquad (3.2)$$

$$B(\ddot{q}) = \begin{bmatrix} \left((m_1 + m_2){l_1}^2 + m_2{l_2}^2 + 2m_2 l_1 l_2 \cos\theta_2\right) & \left(m_2{l_2}^2 - m_2 l_1 l_2 \cos\theta_2\right) \\ \left(m_2{l_2}^2 - m_2 l_1 l_2 \cos\theta_2\right) & m_2{l_2} \end{bmatrix} \qquad (3.2)$$

$$C(\dot{q}, q) = \begin{bmatrix} -m_2 l_1 l_2 \sin\theta_2 \left(2\dot{\theta}_1\dot{\theta}_2 + {\dot{\theta}_2}^2\right) \\ -m_2 l_1 l_2 \sin(\theta_2)\dot{\theta}_1\dot{\theta}_2 \end{bmatrix} \qquad (3.3)$$

$$g(q) = \begin{bmatrix} -(m_1 + m_2) l_1 g \sin\theta_1 - m_2 l_2 g \sin(\theta_1 + \theta_2) \\ -m_2 l_2 g \sin(\theta_1 + \theta_2) \end{bmatrix} \qquad (3.4)$$

$$q = \begin{bmatrix} \theta_1 \\ \theta_1 \end{bmatrix} \qquad (3.5)$$

IV. ROBOT MODELLING AND SIMULATION RESULT

The garri fryer robot was modelled using Autodesk Inventor software and exported to MATLAB/Simulink for the simulation. The developed model is presented in Figure 4.1.

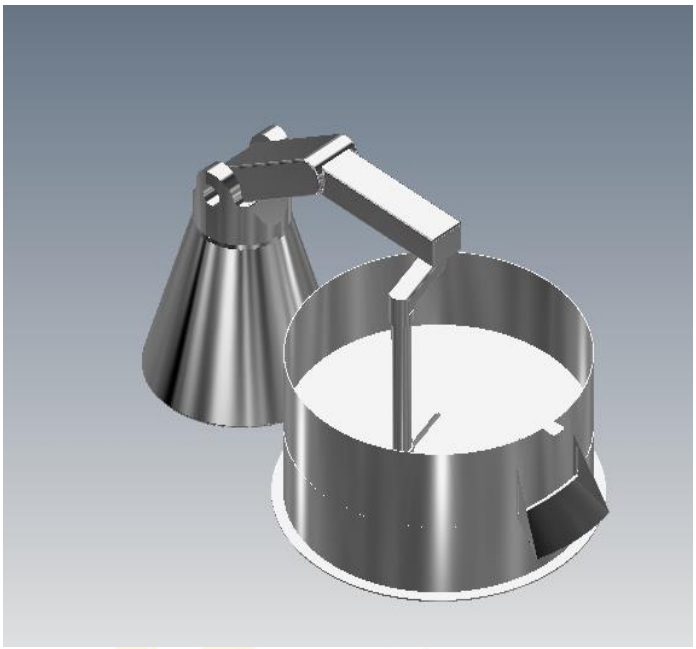

Figure 4.1 CAD Model of the Garri Fryer Robot

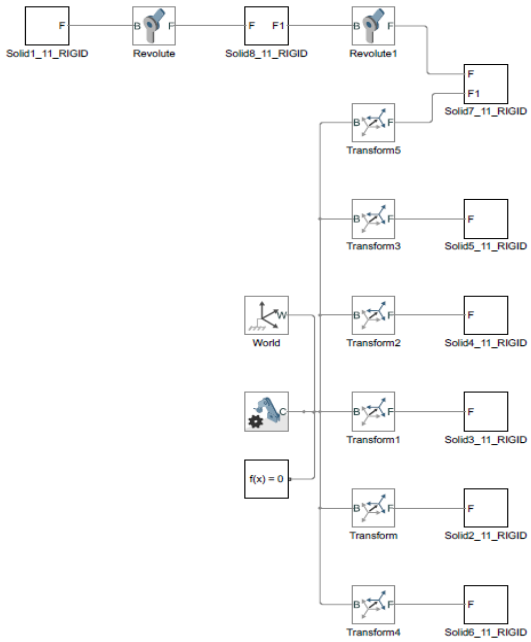

Figure 4.2 Simulink Model of the Garri Fryer

The simulation was done using Simulink. The following components were required:

1. Constant block
2. PID controller
3. PS-Simulink Converter
4. Simulink PS-Converter
5. Controlled Temperature Source
6. Temperature Sensor
7. Thermal Reference
8. Solver Configuration
9. Scope
10. Relay Unit

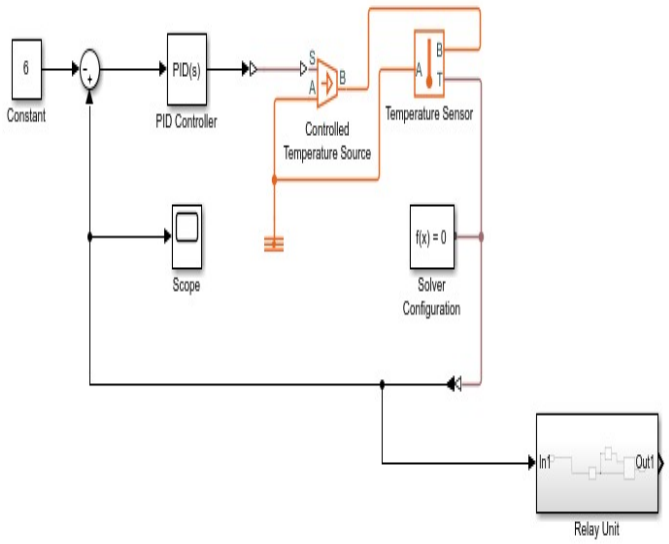

Figure 4.3 Temperature Control Simulation model

As shown in Figure 4.3, a constant is used and the value is set to 6. The constant block is connected to the PID block through the sum block which sums the input and output signals. The PID signal is taken to the Temperature source which reference is set to absolute zero. The output of this temperature source is fed to the temperature sensor for measurement and the measurement result set is fed into MATLAB solver and then the scope for display. Since the system is a closed loop system, the output is fed back for reference and necessary control. An actuator (relay system) is connected to the system output for adequate control (switching on/off) of the temperature source of the garri fryer.

The PID controller was tuned to different values and the resultant waveforms were captured from the scope for the respective values as shown in the Figures 4.4 – 4.7 below. The values of P, I, D, and the time constant were recorded for each plot.

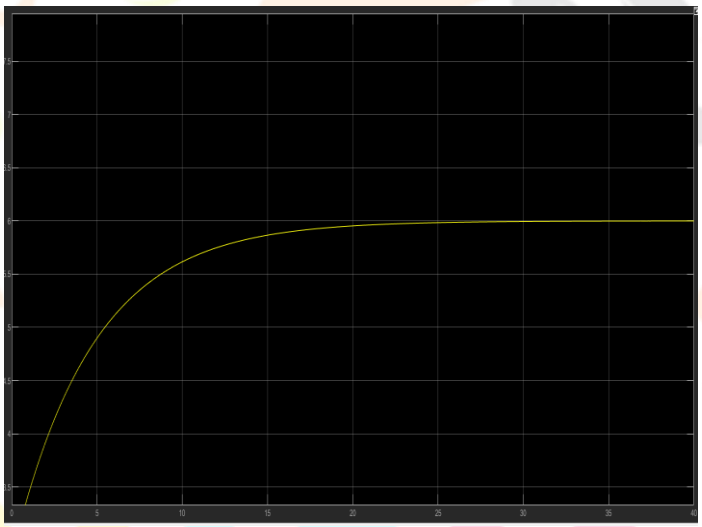

Figure 4.4 Simulink Plot for the temperature controller at P = 0.9, I = 0.4, D = 0.2, t = 40s

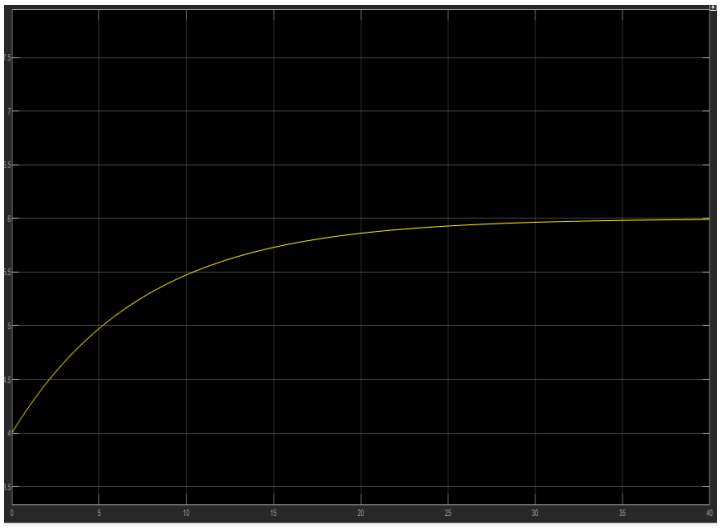

Figure 4.5 Simulink Plot for the temperature controller at P = 2, I = 0.4, D = 0.2, t = 40s

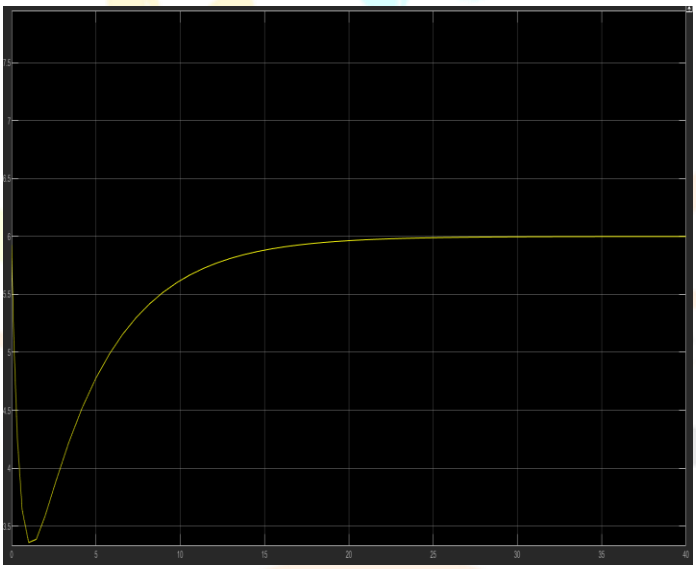

Figure 4.6 Simulink Plot for the temperature controller at P = 0.9, I = 0.4, D = 0.8, t = 40s

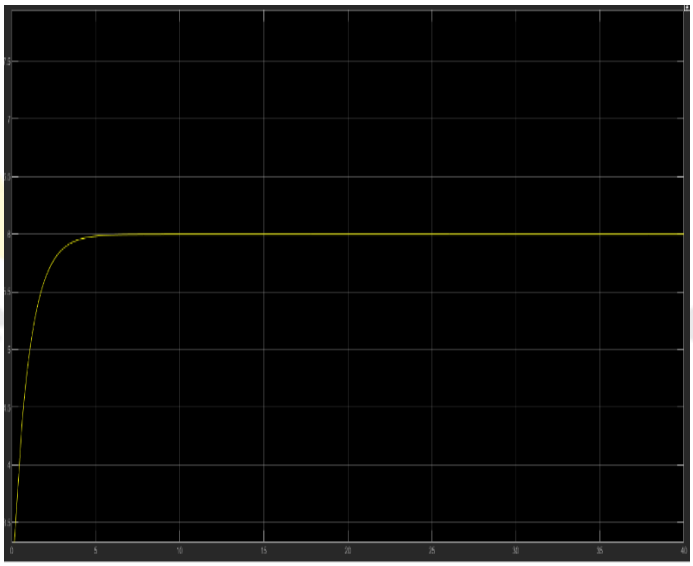

Figure 4.7 Simulink Plot for the temperature controller at P = 0.9, I = 2, D = 0.8, t = 40s

V. DISCUSSION

From the realization of this work, the temperature controller was designed and simulated. The PID gains are manually tuned as shown in Figures 4.4 to 4.7. In Figure 4.4, the Simulink result of the temperature controller at P = 0.9, I = 0.4, D = 0.2, and t = 40s is presented. In Figure 4.5, the Simulink Plot for the temperature controller at P = 2, I = 0.4, D = 0.2, and t = 40s is presented. In Figure 4.6, the Simulink Plot result for the temperature controller at P = 0.9, I = 0.4, D = 0.8, and t = 40s is shown. And in Figure

4.7 the Simulink Plot for the temperature controller at P = 0.9, I = 2, D = 0.8, t = 40s is displayed. This PID gain parameter tuning result conforms with the literature of (Venu Gopal & Shivakumar, 2019a, Premkumar et al., 2019 and Sahu et al., 2021) as different in gain parameters result in a different responses. However, from the evaluation of the result with respect to the reference signal of six (6), Figure 4.4 displayed a settling time of 20secs, Figure 4.5 displayed a settling time of 25secs, and Figure 4.6 displayed a negative slope at 1.6secs and settling time at 19secs, while Figure 4.7, presents a settling time of 4secs. From the results displayed, the most preferred plot with minimal error with respect to the reference signal is Figure 4.7, with the characteristics of a smaller settling time of 4secs (Venu Gopal & Shivakumar, 2019b, Sahu et al., 2021).

Using computer-aided design software, a novel flexible robotic arm for frying cassava into garri was built, and this innovative flexible robotic arm was produced in 3D and simulated using AUTODESK INVENTOR. The robot ran autonomously for about 20 minutes, with the garri being reintroduced into the frying pot at the start of each cycle. The robot spins to a 90-degree angle while in operation, and the paddle makes uniform contact with the frying pot's base. With the controller controlling the motion, the robot made an intermittent 360-degree clockwise and counter-clockwise spin, simulating stirring of the cassava grits (Miriam, 2017; Al-Faraj et al., 2021). The heating system reached 75℃. in the first ten minutes of operation. The grains gelatinized throughout this time of operation. In the next 10 minutes, the temperature climbed to 200℃. After the second ten minutes, the heater was turned off. The temperature regulation of the garri temperature control system was found to be optimal after 20 minutes of operation, which is consistent with the literature of (Onokwai et al., 2019, Onu, 2020, Ovat et al., 2021, Samuel et al., 2021 and Dike et al., 2022) on garri production tolerable temperature to determine an estimated moisture content of 12%. The alarm beeped to indicate that the garri was ready for discharge, and the robotic paddle moved in a clockwise/counter-clockwise pattern for 60 seconds, allowing the fried garri to be discharged more easily. Following the completion of the manufacturing process, the robot arm was raised to its default 90-degree position, allowing another processing cycle to begin. Figure 11 depicts the visualization of the simulation result and the performance analysis; nonetheless, this conforms to the attribute of a robotic arm in (Aljalal et al., 2020, Krishnaraj Rao et al., 2022, Ghodki, 2022, and Ali et al., 2022).

5.1 Conclusion/Recommendation

The temperature regulator was created and simulated, and the report on the design and simulation of a Garri Frying Robotic Arm was completed. The discussion showed the relative validity in relation to important literatures and authorities based on the simulation results. However, this satisfies the presented focus of the study. Hence the following objectives are met. The PID was manually tuned and the preferred tuned gain parameters were presented as **P = 0.9, I = 2, D = 0.8,** which displayed lesser settling time. Also, the robot was designed and modelled in 3D using Arduino Uno micro-controller in AUTODESK INVENTOR. Hence it can be established that the two degree of freedom robotic arm for frying of garri, with regulated temperature can be realized using a PID controller with the presented gain parameters and the Micro-controller in AUTODESK INVENTOR. Following the performance recommended, this automated robotic arm for processing Garri is deemed significant in assisting peasant farmers to process Cassava into Garri with homogenous grits within a short period, reducing the need for manual labor and cost associated with manually producing garri over time.

5.2 Limitation of Study

Further work can be done in the realization of the physical model of this robotic garri fryer. Also, the PID gain parameters can be tuned using a metaheuristic or heuristic algorithm to ensure the optimal gain parameters.

REFERENCES

[1] Adesope, A., Olumide-Ojo, O., Oyewo, I. O., Ugege, B. H., & Oyelade, A. A. (2020). Economic Analysis of Cassava Flour and Garri Production in Ibarapa Local Government Area, Oyo State, Nigeria. Journal of Applied Sciences and Environmental Management, 24(9), 1551–1554. https://doi.org/10.4314/jasem.v24i9.11

[2] Al-Faraj, S., Al-Bahrani, M., Al-Ghamdi, S., Rafie, M., Bashar, A., & Latif, G. (2021). CNN-Based Alphabet Identification and Sorting Robotic Arm. Lecture Notes in Electrical Engineering, 733 LNEE, 349–362. https://doi.org/10.1007/978-981-33-4909-4_26

[3] Ali, H. M., Hashim, Y., & Al-Sakkal, G. A. (2022). Design and implementation of Arduino based robotic arm. International Journal of Electrical and Computer Engineering, 12(2), 1411–1418. https://doi.org/10.11591/ijece.v12i2.pp1411-1418

[4] Aljalal, M., Ibrahim, S., Djemal, R., & Ko, W. (2020). Comprehensive review on brain-controlled mobile robots and robotic arms based on electroencephalography signals. In Intelligent Service Robotics (Vol. 13, Issue 4, pp. 539–563). Springer Science and Business Media Deutschland GmbH. https://doi.org/10.1007/s11370-020-00328-5

[5] Charles Nnaji, C., & Chigozie Akanno, C. (2022). Assessment Of Environmental Degradation Due To Processing Of Cassava Into Garri Flakes. https://doi.org/10.21203/rs.3.rs-1346609/v1

[6] Dike, K. S., Okafor, C. P., Ohabughiro, B. N., Maduwuba, M. C., Ezeokoli, O. T., Ayeni, K. I., Okafor, C. M., & Ezekiel, C. N. (2022). Analysis of bacterial communities of three cassava-based traditionally fermented Nigerian foods (abacha, fufu and garri). Letters in Applied Microbiology, 74(3), 452–461. https://doi.org/10.1111/lam.13621

[7] Falanga, D., Kleber, K., & Scaramuzza, D. (2020). Dynamic obstacle avoidance for quadrotors with event cameras. Science Robotics, 5(40). https://doi.org/10.1126/scirobotics.aaz9712

[8] Ghodki, M. K. (2022). A new solar powered robotic arm guided master–slave electric motors of biomass conveyor. Journal of Engineering, Design and Technology. https://doi.org/10.1108/jedt-09-2021-0496

[9] Kayode, *, Adebayo, A. O., Awoyemi, S. A., & Oyeniran, A. O. (2021). Utilization of Garri-Processing Methods among Rural Women in Iwo Local Government Area, Osun State, Nigeria. JAFE, 8(2), 1–10. https://uilspace.unilorin.edu.ng/handle/20.500.12484/7375

[10] Krishnaraj Rao, N. S., Avinash, N. J., Rama Moorthy, H., Karthik, K., Rao, S., & Santosh, S. (2022). An Automated Robotic Arm: A Machine Learning Approach. Ieeexplore.Ieee.Org, 1–6. https://doi.org/10.1109/icmnwc52512.2021.9688512

[11] Miriam, N. M. (2017). Improved production technologies and cultural practices used by cassava producers in Enugu State, Nigeria. Idosr.Org, 2(1), 93–112. https://www.idosr.org/wp-content/uploads/2021/07/IDOSR-JBESS-21-93-112-2017-1.pdf

[12] Ndife, J. (2019). Effect of palm oil inclusion on the quality of garri produced from white and yellow cassava (Manihot esculenta cranz) roots (Manihot esculenta cranz) roots. International Journal of Food Science and Nutrition, 4(3), 180–185. https://www.researchgate.net/profile/Joel-Ndife/publication/333852609_Effect_of_palm_oil_inclusion_on_the_quality_of_garri_produced_from_white_and_yellow_cassava_Manihot_esculenta_cranz_roots/links/5d08f5b692851cfcc620e867/Effect-of-palm-oil-inclusion-on-

[13] Nwadinobi, C., Edeh, J., & Mejeh, K. I. (2019). Design and Development of a Vertical Paddle Semi Automated Garri Frying Machine. Journal of Applied Sciences and Environmental Management, 23(7), 1279. https://doi.org/10.4314/jasem.v23i7.14

[14] Onokwai, A. O., Okonkwo, U. C., Osueke, C. O., Ezugwu, C. A., Eze, N. C., Diarah, R. S., & Olawale, O. (2019). Quantifying cassava waste generation and biogas production in eHa-alumona grinding mills. International Journal of Civil Engineering and Technology, 10(1), 2032–2043. http://eprints.lmu.edu.ng/2287/

[15] Onu, U. G. (2020). Design of Garri Frying Machine with User-defined Temperature Regulation and Motion Control System. International Journal for Research in Applied Science and Engineering Technology, 8(8), 1584–1589. https://doi.org/10.22214/ijraset.2020.31205

[16] Ovat, F., Nyong, O., & Adie, J. (2021). DEVELOPMENT OF A MOTORIZED VIBRATORY SIEVING MACHINE FOR IMPROVED GARRI PRODUCTION. Researchgate.Net. https://www.researchgate.net/profile/A-J-Anyandi-2/publication/356493022_DEVELOPMENT_OF_A_MOTORIZED_VIBRATORY_SIEVING_MACHINE_FOR_IMPROVED_GARRI_PRODUCTION/links/619df16c3068c54fa519b60b/DEVELOPMENT-OF-A-MOTORIZED-VIBRATORY-SIEVING-MACHINE-FOR-IMPROVED-GARRI-PRODUCTION.pdf

[17] Pradhan, A. A., Martin, W. C., Ruiz, J. D., & Deierling, P. E. (2021). Framework for automated robotic arm manipulation in variable industrial environments. ASME International Mechanical Engineering Congress and Exposition, Proceedings (IMECE), 2B-2021. https://doi.org/10.1115/IMECE2021-71479

[18] Premkumar, K., Thamizhselvan, T., Vishnu Priya, M., Ron Carter, S. B., & Sivakumar, L. P. (2019). Fuzzy anti-windup pid controlled induction motor. International Journal of Engineering and Advanced Technology, 9(1), 184–189. https://doi.org/10.35940/ijeat.A1113.109119

[19] Sahu, A., Mohanty, K. B., & Mishra, R. N. (2021). Development and experimental realization of an adaptive neural-based discrete model predictive direct torque and flux controller for induction motor drive. Applied Soft Computing, 108. https://doi.org/10.1016/j.asoc.2021.107418

[20] Samuel, A. U., Akinlabi, E. T., Okokpujie, I. P., & Fayomi, O. S. I. (2021). Sustainability of Garri Processing: A Case Study of Ogun State, Nigeria. IOP Conference Series: Materials Science and Engineering, 1107(1), 012132. https://doi.org/10.1088/1757-899x/1107/1/012132

[21] Tsai, Y. T., Lee, C. H., Liu, T. Y., Chang, T. J., Wang, C. S., Pawar, S. J., Huang, P. H., & Huang, J. H. (2020). Utilization of a reinforcement learning algorithm for the accurate alignment of a robotic arm in a complete soft fabric shoe tongues automation process. Journal of Manufacturing Systems, 56, 501–513. https://doi.org/10.1016/j.jmsy.2020.07.001

[22] Venu Gopal, B. T., & Shivakumar, E. G. (2019a). Design and simulation of neuro-fuzzy controller for indirect vector-controlled induction motor drive. In Lecture Notes in Networks and Systems (Vol. 43, pp. 155–167). Springer. https://doi.org/10.1007/978-981-13-2514-4_14

[23] Venu Gopal, B. T., & Shivakumar, E. G. (2019b). Design and simulation of neuro-fuzzy controller for indirect vector-controlled induction motor drive. In Lecture Notes in Networks and Systems (Vol. 43, pp. 155–167). https://doi.org/10.1007/978-981-13-2514-4_14

[24] Vestartas, P., & Weinand, Y. (2020). Laser Scanning with Industrial Robot Arm for Raw-wood Fabrication. Proceedings of the 37th International Symposium on Automation and Robotics in Construction, ISARC 2020: From Demonstration to Practical Use - To New Stage of Construction Robot, 773–780. https://doi.org/10.22260/isarc2020/0107

[25] Wang, D., Lutz, B., Cobb, P. J., & Dames, P. (2021). RASCAL: Robotic Arm for Sherds and Ceramics Automated Locomotion. Ieeexplore.Ieee.Org, 6378–6384. https://doi.org/10.1109/icra48506.2021.9561057

[26] Wu, A., Tong, W., Dwyer, T., Lee, B., Isenberg, P., & Qu, H. (2021). MobileVisFixer: Tailoring Web Visualizations for Mobile Phones Leveraging an Explainable Reinforcement Learning Framework. IEEE Transactions on Visualization and Computer Graphics, 27(2), 464–474. https://doi.org/10.1109/TVCG.2020.3030423